Mathematical Modeling and Optimization of Tribological Behaviour of Al 7075 Based Hybrid Nanocomposites

Kannan C[1*], Ramanujam R[2] and Balan A S S[3]

[1,2] School of Mechanical Engineering, Vellore Institute of Technology, Vellore, Tamilnadu

[3] Department of Mechanical Engineering, NIT Surathkal, Karnataka, India

* Corresponding author
Email: kannan.chidambaram@vit.ac.in

Abstract

Many industrial applications necessitate lightweight materials that possess better tribological behaviour. Whilst aluminium based nanocomposites are proposed owing to their lightness, their tribological characteristics must be improved which are dominantly influenced by the selection of reinforcements, manufacturing process and heat treatments. In this research, an aluminium hybrid nanocomposite is produced using a novel molten salt processing and subjected to different heat treatments. Their tribological behaviour is assessed under different operating conditions viz. load, sliding velocity and material condition of the pin. Regression models are formulated to predict the tribological behaviour of developed hybrid composite under different heat treatments. The most significant parameter and optimum level for each of these operating parameters are determined using analysis of variance, main and interaction plots and response surface methodology in the end. The integrated approach helps in deciding the optimum parameter setting for the development of nanocomposite with ameliorated tribological behaviour. Under the optimized conditions, the hybrid nanocomposite could able to reduce the wear resistance by about 63% and the coefficient of friction by 18.5% than unreinforced alloy.

Keywords: molten salt processing, nanocomposite, optimization, tribological, response surface methodology, desirability etc.

1. Introduction

All industrial applications demand the equipment of improved reliability, efficiency and mass reduction as well. These demands are currently met with the usage of metal matrix composites. Lightness and durability along with good corrosion resistance make aluminium as most popular for the development of composites. Improved fracture toughness and ductility

substantiate the selection of nanocomposites and nanoparticle inclusion improves the mechanical and wear-resistant characteristics of the matrix [1].

The industrial equipment that constitutes a pair of working surfaces requires improved mechanical and wear-resistant properties in addition to self-lubrication. This could be achieved with the incorporation of two different types of nanoparticles into an aluminium matrix [2]. Among these nanoparticles, one must provide self-lubrication characteristics, while another is contributing to improved mechanical properties. The development of novel hybrid nanocomposites fulfilling the above requirements is a time of concern.

Muley et al. [3] fabricated an aluminium alloy based hybrid composites through stir casting process using 1 wt.% SiC and 1 wt.% Al_2O_3 nanoparticles. Preheated reinforcements were added to the melt and stirred at 400-600 rpm. Thus produced hybrid nanocomposite ensued an increase of 17% in Vickers hardness and 39% in ultimate tensile strength. Moreover, wear loss was reduced by 80% in the hybrid nanocomposite.

El-Mahallawi et al. [4] developed A356 based nanocomposite using Al_2O_3 particles. Nano-Al_2O_3 particles were added to the matrix in different weight fraction (0-5 %) and variable stirring speeds (270, 800, 1500 and 2150 rpm) were adopted both in the semisolid and liquid state. Improved hardness, ultimate tensile strength and elongation were reported for 2 wt. % nano-Al_2O_3 reinforced composite produced at a stirring speed of 1500 rpm in semisolid state.

The effect of Al_2O_3 nanoparticles addition and subsequent extrusion process on Al 6061 was investigated [5]. Milled nano Al_2O_3/Al composite powder was injected using an inert gas and followed by mechanical stirring. The mechanical properties of composites increased up to 1 wt. % of Al_2O_3 and beyond 1.5 wt. %, they started to decrease. Increased porosity and agglomeration of nanoparticles with higher weight fraction was reported for this declining trend. The porosity was brought down by an extrusion process.

Su et al. [6] produced AA2024/nano Al_2O_3 composites by semisolid casting with ultrasonic treatment. Refined grain structure, homogeneous distribution of nanoparticles and low porosity were observed with the developed composites. While comparing with aluminium alloy, an improvement of 81 % in yield strength was reported for 1 wt. % nano Al_2O_3 reinforced composite.

The mechanical and tribological tests carried out on Al 7075-TiC composites fabricated by incorporating 2-10 wt.% of TiC particulates revealed relatively higher hardness, tensile strength and elongation under both as-cast and artificially aged conditions. Dry sliding wear tests were conducted on composites revealed improved wear resistance of composites up to 8

wt.% of TiC particles. The artificially aged composites were displaying better wear resistance over as-cast composites [7].

Iacob et al. [8], Baradeswaran and Perumal [9] have established that embedding the graphite particulates in the aluminium matrix improved their tribological behaviour substantially. The improved tribological properties of the manufactured composites are attributed to the presence of graphite, a solid lubricant. A continuous graphite film was established at the contact surface after the initial run-in period due to extensive deformation and fragmentation of graphite during the sliding contact. This film provides a hindrance for metal to metal contact and thus prevents seizure. However, the graphite reinforced composites are possessing inferior mechanical properties when compared to unreinforced aluminium alloy.

Chen et al. [10] developed the hexagonal boron nitride (h-BN) reinforced al matrix composite using a semisolid powder metallurgy technique. An inverse relationship was observed between compressive strength and powder size. The sliding friction behaviour of Al 7075 based composites with various born containing particles was analyzed [11]. Lower wear spot and intensity was observed for composites that contain h-BN.

Improved mechanical and tribological characteristics of nanocomposites necessitate the uniform nanoparticle distribution within the matrix. The nanocomposites produced by conventional stir casting were not able to prevent the agglomeration of nanoparticles which finally impaired the quality of composite castings. This issue was reported by the majority of researchers who developed the nanocomposites through a mechanical stir casting process. In recent times, ultrasonic cavitation and molten salt processed composites are attracting the researcher's attention due to their ability to overcome the agglomeration effect [12-15].

During the development of aluminium based nanocomposites, hybridization of reinforcement becomes universal owing to their benefits over single particle reinforced composites [16,17]. This technique renders the path of overcoming the drawbacks imposed by single hard ceramic particle reinforced composites such as poor machinability characteristics [18]. The load bearing capacity of Al_2O_3 [19] and self-lubricating properties of h-BN [20] are well established. To the best of author's knowledge, there has been little exploration on the tribological behavioural assessment of hybrid nanocomposite that involves hard ceramic Al_2O_3 and soft self-lubricating BN particles. The impact of heat treatment especially the deep cryogenic treatment on tribological characteristics of hybrid nanocomposite needs further exploration, as revealed by the literature survey. Hence, the objectives of this research work are (i) to explore the influence of heat treatment and processing method on the tribological

behaviour (ii) to develop mathematical models and (iii) to optimize the input parameters for the enhancement of tribological characteristics of nanocomposite using different approaches.

2. Materials and Methods

In this work, Al 7075 based hybrid composite with the incorporation of 1wt. % Al_2O_3 and 0.5 wt.% BN nanoparticles was produced by a molten salt processing which was elaborately detailed in the authors' previous works [12,13]. This manufacturing method involves several stages viz. (a) mixing of reinforcements (Al_2O_3 and h-BN) with molten fluoride salts ($KAlF_4$), (b) dehydration of mixture using vacuum furnace, (c) loading of the dehydrated mixture on the surface of molten aluminium, (d) ultrasonic agitation, (e) optimized mechanical stirring and finally (f) squeeze-casting at 150 MPa. The set up used for the manufacturing of squeeze-cast hybrid nanocomposite is shown in Fig 1. The set up is consisted of a bottom pouring type stir casting furnace (0-2 kg) coupled with a squeeze casting attachment (0-150 MPa) and ultrasonic vibrator (20 kHz, 1 kW). Thus, produced hybrid nanocomposites were further subjected to different heat treatments viz. artificial ageing (T_6) and deep cryogenic treatment (DCT).

Fig 1. Experimental Set up

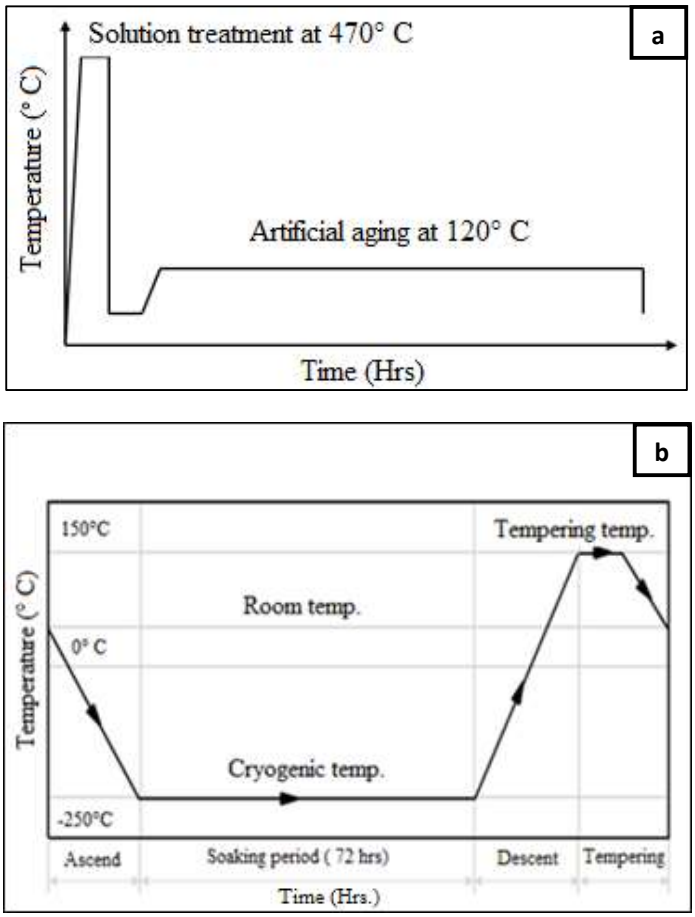

Fig 2. Schematic of processing cycle for (a) T_6 (b) DCT

The processing cycle adopted for T_6 and DCT is schematically presented in Fig 2a and Fig 2b. A tubular furnace and an electric oven (Delta Power Controls, Bangalore) were used in T_6; while the cryo box with liquid nitrogen supply was used in DCT. The unreinforced alloy and molten salt processed hybrid nanocomposite were further subjected to T_6 and DCT. The influence of heat treatment on mechanical properties of molten salt processed hybrid nanocomposite was investigated and the results are presented in Table 1.

Table 1. Mechanical properties of molten salt processed hybrid nanocomposite under the influence of different heat treatments

Properties	Heat treatment		
	As-cast	**T_6**	**DCT**
Ultimate tensile strength (MPa)	239	496	255
% elongation	2.6	6.2	2.8
Young's modulus (GPa)	68.7	72.7	70.6
Vicker hardness (HV)	154	215	167
Impact energy absorbed (J)	5.9	21.8	6.4

The molten salt processed hybrid nanocomposites are further subjected to tribological investigation. For this purpose of tribological characterisation, dry sliding wear tests are carried out using a pin-on-disk wear testing machine (TR 20LE, DUCOM) according to ASTM G99-05 standards. The different levels of load, sliding velocity and the material condition of composite pin considered in this study are presented in Table 2. A total of 54 square pins with dimensions of 4.5mm x 4.5mm x 30 mm are machined from the casted samples and polished. The samples are subjected to T_6 and DCT treatments to study their influence on wear behaviour. During the test, these pins are made to press against a rotating hardened steel disc (60-70 HRC). This is achieved by applying a load that acts as a counterweight and balances the pin. This was done to optimize the operating conditions and to develop the mathematical models to predict the wear behaviour of the hybrid nanocomposite. Scanning electron microscope (SEM) is used to identify the dominant wear mechanisms in unreinforced alloy and hybrid nanocomposite.

3. Results and Discussion

3.1. Mathematical Modelling and Optimization

The modelling of wear behaviour of unreinforced alloy and hybrid composite was carried out using the MINITAB17 software. The different factors with their levels for the tribological experiments are presented in Table 2. The tests were performed with pins made of unreinforced alloy and hybrid nanocomposite under different heat treatments. From these observations, the specific wear rate (SWR) and the coefficient of friction (CoF) were determined for different material samples.

Table 2. Factors and their levels for a wear test

Sl.No	Factors	Levels		
		Low (-1)	**Medium (0)**	**High (1)**
1	Load, L (N)	10	20	30
2	Sliding velocity, V (m/s)	0.5	1.0	1.5
3	Material condition, C	1(as cast)	2 (T_6)	3 (DCT)

Table 3 shows the responses (SWR and CoF) of unreinforced aluminium alloy and hybrid nanocomposites for different levels of load, sliding velocity and material condition of the pin.

Table 3. Response table for independent variables in unreinforced alloy and hybrid nanocomposite

Load	Sliding	Material	Unreinforced alloy		Hybrid nanocomposite	
(N)	Velocity (m/s)	Condition	SWR (mm^3/m)	COF	SWR(mm^3/m)	COF
10	0.5	1	0.0155000	0.324	0.0128827	0.302
10	0.5	2	0.0099840	0.294	0.0094016	0.288
10	0.5	3	0.0154724	0.318	0.0103610	0.296
10	1.0	1	0.0132936	0.317	0.0063043	0.296
10	1.0	2	0.0087429	0.302	0.0057561	0.278
10	1.0	3	0.0149484	0.310	0.0098128	0.290
10	1.5	1	0.0113078	0.309	0.0049338	0.286
10	1.5	2	0.0073363	0.298	0.0041937	0.267
10	1.5	3	0.0089911	0.302	0.0059480	0.271
20	0.5	1	0.0270836	0.377	0.0167201	0.358
20	0.5	2	0.0154448	0.327	0.0141436	0.321
20	0.5	3	0.0255115	0.363	0.0163912	0.354
20	1.0	1	0.0207402	0.353	0.0119782	0.302
20	1.0	2	0.0149484	0.310	0.0104706	0.298
20	1.0	3	0.0150035	0.324	0.0111011	0.301
20	1.5	1	0.0154724	0.316	0.0080311	0.284
20	1.5	2	0.0099288	0.292	0.0059480	0.271
20	1.5	3	0.0104528	0.296	0.0064139	0.276
30	0.5	1	0.0317722	0.412	0.0191870	0.375
30	0.5	2	0.0255942	0.364	0.0176657	0.362
30	0.5	3	0.0299243	0.393	0.0189403	0.372
30	1.0	1	0.0306138	0.394	0.0156237	0.333
30	1.0	2	0.0175685	0.357	0.0134309	0.321
30	1.0	3	0.0257046	0.368	0.0144177	0.327
30	1.5	1	0.0248220	0.363	0.0131568	0.321
30	1.5	2	0.0170996	0.336	0.0112381	0.302
30	1.5	3	0.0204092	0.341	0.0122523	0.312

The relationship between response variable y, and predictor variables can be established using a multiple linear regression model as shown in eqn. (1)

$$y = \beta_0 + \beta_i(A_i) + \beta_2(B_i) + \beta_3(C_i) + .. \beta_i(A_i * B_i) .. + .. \beta_i(A_i * C_i) .. + .. \beta_i(B_i * C_i) .. + \mathcal{E}_i \quad (1)$$

Here, ε_i - deviations, y - response variable, β_i - regression coefficients. A, B and C – predictor variables (load, sliding velocity and material condition), i – the levels of predictor variables. Considering the interaction terms up to second-order, the regression models are developed and presented in Table 4.

Table 4. Regression models for response variables in unreinforced alloy and hybrid nanocomposite

Response	Regression Equation	R^2 (%)	R^2_{adj} (%)	R^2_{pred} (%)
Unreinforced alloy				
Specific wear rate (mm^3/m)	0.02789 + 0.000581*L - 0.00073*V - 0.02126*C + 0.000011*L*L - 0.00023*V*V + 0.005763*C*C - 0.000194*L*V - 0.000087*L*C - 0.00138*V*C	94.2	91.2	86.6
CoF	0.3770 + 0.00143*L + 0.0219* V - 0.0922*C + 0.000103* L*L - 0.0100*V*V + 0.02333*C*C - 0.001700*L*V - 0.000392*L*C - 0.00167 V*C	94.4	91.4	87.0
Hybrid composite				
Specific wear rate (mm^3/m)	0.01794 + 0.000398*L - 0.01152* V - 0.00637*C + 0.000002*L*L + 0.00223*V*V+ 0.001664*C*C - 0.000026*L*V - 0.000036*L*C + 0.000265*V*C	95.9	93.9	88.9
CoF	0.3547 + 0.00269*L - 0.0610*V - 0.0549*C + 0.000038*L*L + 0.0280*V*V + 0.01333*C*C - 0.001867*L*V + 0.000075*L*C - 0.00317 V*C	94.1	91.0	84.7

3.2. Analysis of Variance (ANOVA) for Factorial Design of Experiments

ANOVA is employed in this investigation to determine the influence of input factors on the output responses namely specific wear and COF of unreinforced alloy and hybrid nanocomposite. As this research work involves three factors with three levels, several hypotheses must be made and tested. At least, one hypothesis for each main factor and one for interaction effect is mandatory for each category of the material.

The null hypothesis for each of the factors considered in this investigation is 'there is no significant difference in SWR / CoF' while increasing the level of the factor. For the interaction factor, the null hypothesis would be 'no interaction between the factors'. Table 5 (a-b) shows the ANOVA for SWR and CoF of unreinforced alloy while Table 5 (c-d) is showing ANOVA for hybrid nanocomposite. P-values (α level of 0.05) were used to decide whether factor data was statistically significant to reject the null hypothesis. The main factors were found to have a significant effect on the SWR and CoF of unreinforced alloy and hybrid nanocomposite. It can be inferred from table 5(a-d). Interactions of the factors did not seem to affect SWR but, load and sliding velocity condition interaction effect was found to be significant on the CoF of both materials under investigation.

Table 5 (a) ANOVA for specific wear rate of unreinforced alloy

Source	Degree of freedom (DF)	Adj. Sum of squares (SS)	Adj. mean squares (MS)	F-value	P-value
Load	2	0.000780	0.000390	87.03	0.000
Sliding velocity	2	0.000276	0.000138	30.78	0.000
Material condition	2	0.000232	0.000116	25.86	0.000
Load *sliding velocity	4	0.000032	0.000008	1.80	0.221
Load *material condition	4	0.000020	0.000005	1.13	0.406

Sliding velocity*material condition	4	0.000018	0.000005	1.03	0.447
Error	8	0.000036	0.000004		
Total	26	0.001395			

(b) ANOVA for COF of unreinforced alloy

Source	**Degree of freedom (DF)**	**Adj. Sum of squares (SS)**	**Adj. mean squares (MS)**	**F-value**	**P-value**
Load	2	0.017692	0.008846	1460.77	0.000
Sliding velocity	2	0.005691	0.002845	469.89	0.000
Material condition	2	0.004517	0.002258	372.94	0.000
Load *sliding velocity	4	0.001689	0.000422	69.72	0.000
Load *material condition	4	0.000424	0.000106	17.50	0.001
Sliding velocity*material condition	4	0.000616	0.000154	25.45	0.000
Error	8	0.000006			
Total	26	0.030677			

(c) ANOVA for specific wear rate of hybrid nanocomposite

Source	**Degree of freedom (DF)**	**Adj. Sum of squares (SS)**	**Adj. mean squares (MS)**	**F-value**	**P-value**
Load	2	0.000245	0.000122	111.26	0.000
Sliding velocity	2	0.000226	0.000113	103.02	0.000
Material condition	2	0.000017	0.000009	7.82	0.013
Load *sliding velocity	4	0.000009	0.000002	2.04	0.182
Load * material condition	4	0.000003	0.000001	0.58	0.683
Sliding velocity*material condition	4	0.000002	0.000001	0.50	0.734
Error	8	0.000009	0.000001		
Total	26	0.000511			

(d) ANOVA for COF of hybrid nanocomposite

Source	**Degree of freedom (DF)**	**Adj. Sum of squares (SS)**	**Adj. mean squares (MS)**	**F-value**	**P-value**
Load	2	0.011388	0.005694	155.06	0.000
Sliding velocity	2	0.010952	0.005476	149.12	0.000
Material condition	2	0.001254	0.000627	17.07	0.001
Load *sliding velocity	4	0.002140	0.000535	14.57	0.001
Load *material condition	4	0.000036	0.000009	0.25	0.904
Sliding velocity*material condition	4	0.000148	0.000037	1.01	0.456
Error	8	0.000294	0.000037		
Total	26	0.026213			

3.3. Main and Interactions effect plot

Fig. 3a and 3b show the main effects plot for the different levels of load, sliding velocity and pin material condition on the SWR and CoF of the unreinforced alloy. The deviation from the mean response with the variations in the levels of a factor can be determined from the main

effects plot. In other words, it is the change in SWR and CoF when the levels of load, sliding velocity and material condition are changed. A large deviation between the maximum and minimum value with that of average indicates that the output response is largely influenced by a change in the level of the factor. It can be inferred from Fig 3a that the factor load has the dominant effect followed by the sliding velocity and material condition of the pin in influencing the SWR. A similar trend is observed for CoF of unreinforced alloy, which is shown in Fig 3b. For hybrid nanocomposite, both load and sliding velocity are found to be influencing the SWR and CoF; while the material condition has an insignificant effect. This is shown in Fig 4(a-b).

ANOVA results suggested that there could be a strong interaction between load and sliding velocity; hence the interaction plots for SWR and CoF of both materials are to be examined. Fig. 3(c-d) and Fig 4(c-d) shows the interaction plots for SWR and CoF for the materials under investigation. The influence of different combinations of load, sliding velocity and material condition on SWR and CoF are depicted in interaction plots. The interaction among the factors is manifested when the slopes of lines are different. Higher influence on SWR and CoF for both materials was observed at low applied load (10N) and higher sliding velocity (1.5 m/s) due to the interactions present. No significant interactions were observed between the sliding velocity and the material condition.

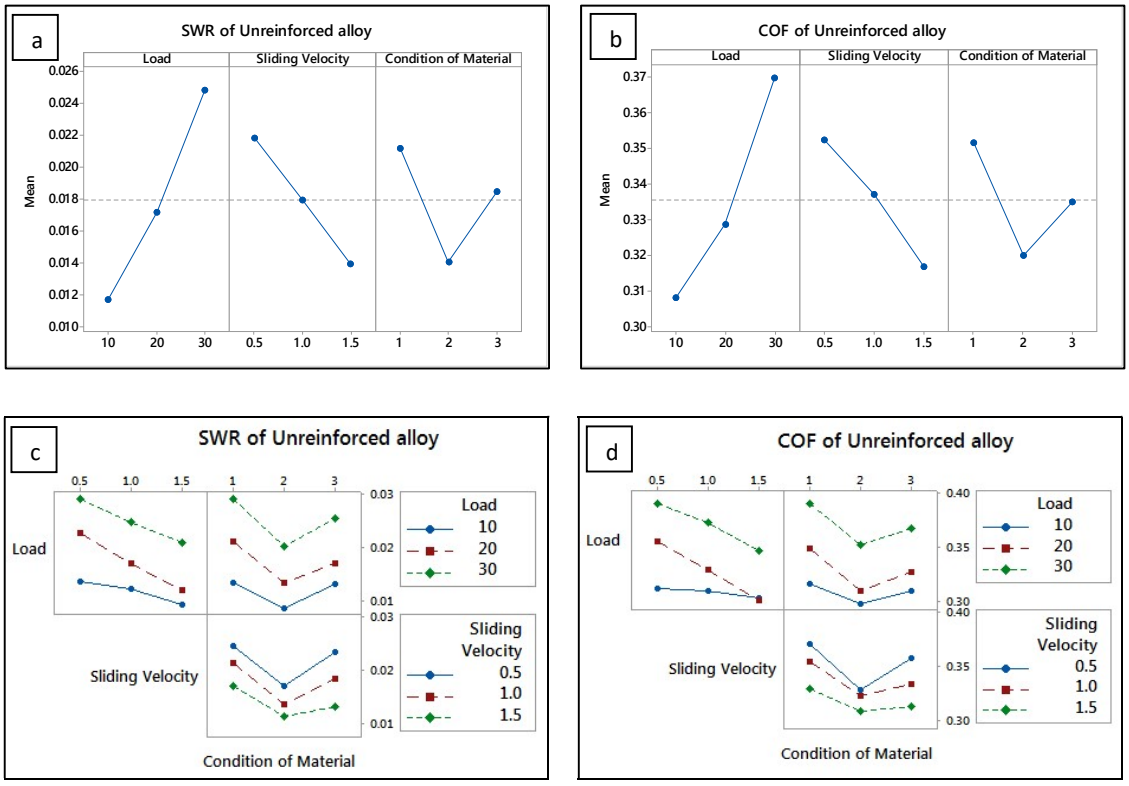

Fig 3 (a-b) Main effects plot (c-d) interaction effects plot for unreinforced alloy

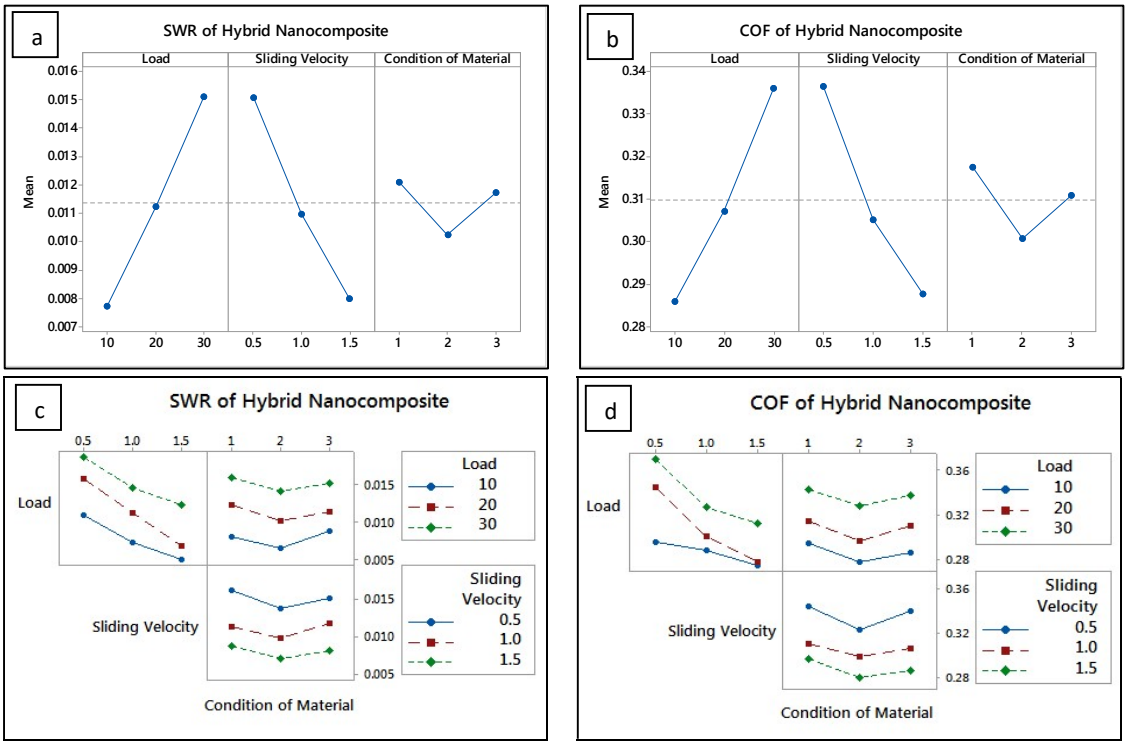

Fig 4 (a-b) Main effects plot (c-d) interaction effects plot for hybrid nanocomposite

3.4. Checking of data and adequacy of the model

Using the normality plot, the exactness of measured data can be checked. The normal probability plot of the output responses SWR and CoF generated for investigated materials is shown in Fig 5. The normal distribution of errors is indicated by the residuals falling on the straight line. ANOVA endorses the significance of the developed model. The values of the determination coefficient R^2 for SWR (94.2%) and CoF (94.4%) of unreinforced alloy show the high significance of the model. The corresponding determination coefficient values of 95.9% and 94.1% are observed for hybrid nanocomposite. The ANOVA results shown in Table 4 for SWR and CoF of unreinforced alloy and hybrid nanocomposite suggest that the predictability of the model is at 95% confidence level because the P is 0.001.

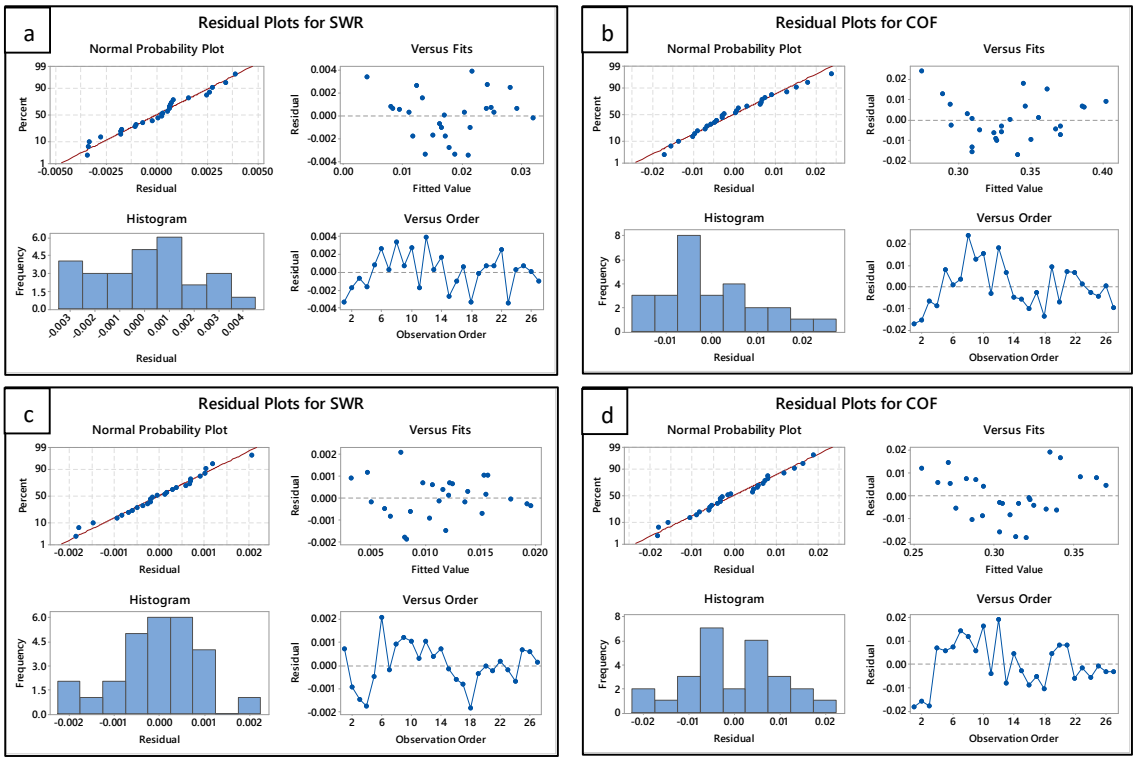

Fig 5. Input data analysis of (a) SWR of unreinforced Al 7075 alloy, (b) CoF of unreinforced Al 7075 alloy, (c) SWR of Al 7075 hybrid nanocomposite and (d) CoF of Al 7075 hybrid composite.

3.5. Optimization

In this research, the optimization is carried out on the objective 'smaller is the better concept'. Hence, the optimum conditions are set as low for output responses (SWR and CoF). Using Minitab software, the 2D contour maps were developed and these could be utilized to identify the various regions in the mechanism with corresponding colour changes in the contour plot. The contour plots were developed for load, sliding velocity and material condition for the corresponding output responses of unreinforced alloy and hybrid nanocomposite. The graphical representation for 2D contour plots for aluminium alloy and composite is shown in Fig 6 and 7 respectively.

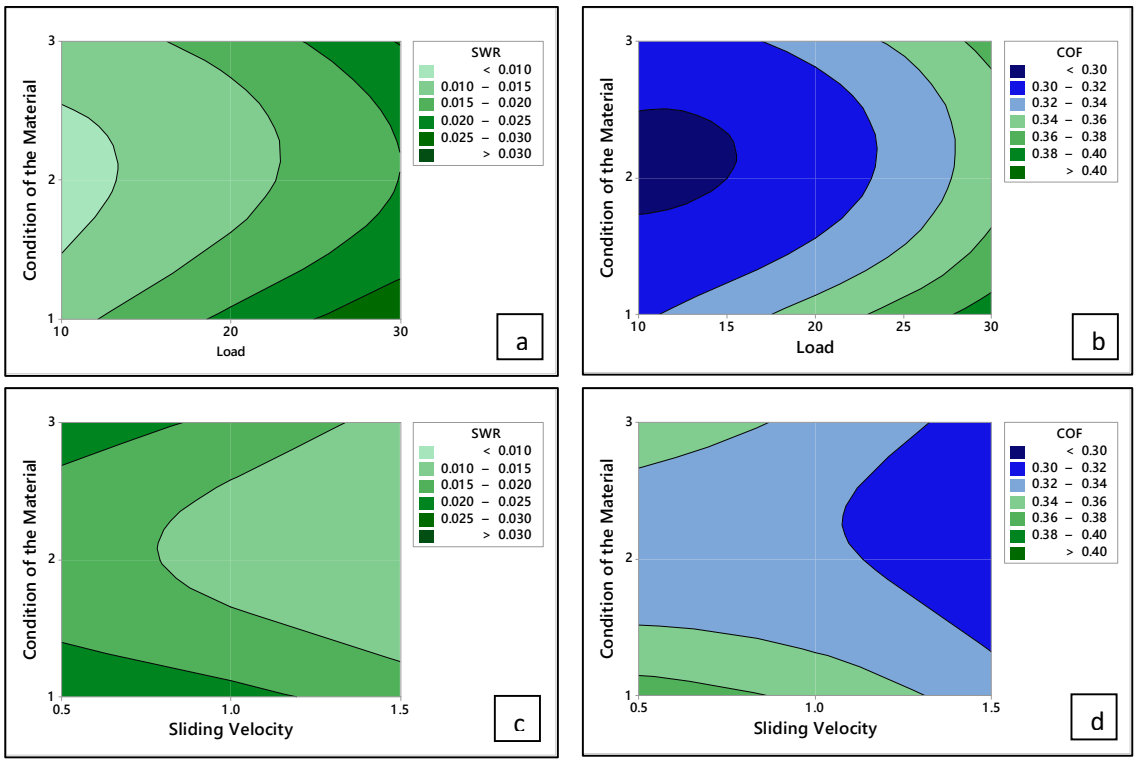

Fig 6. Variations in output responses of unreinforced alloy (a-b) with respect to applied load and material condition (c-d) with respect to velocity and material condition

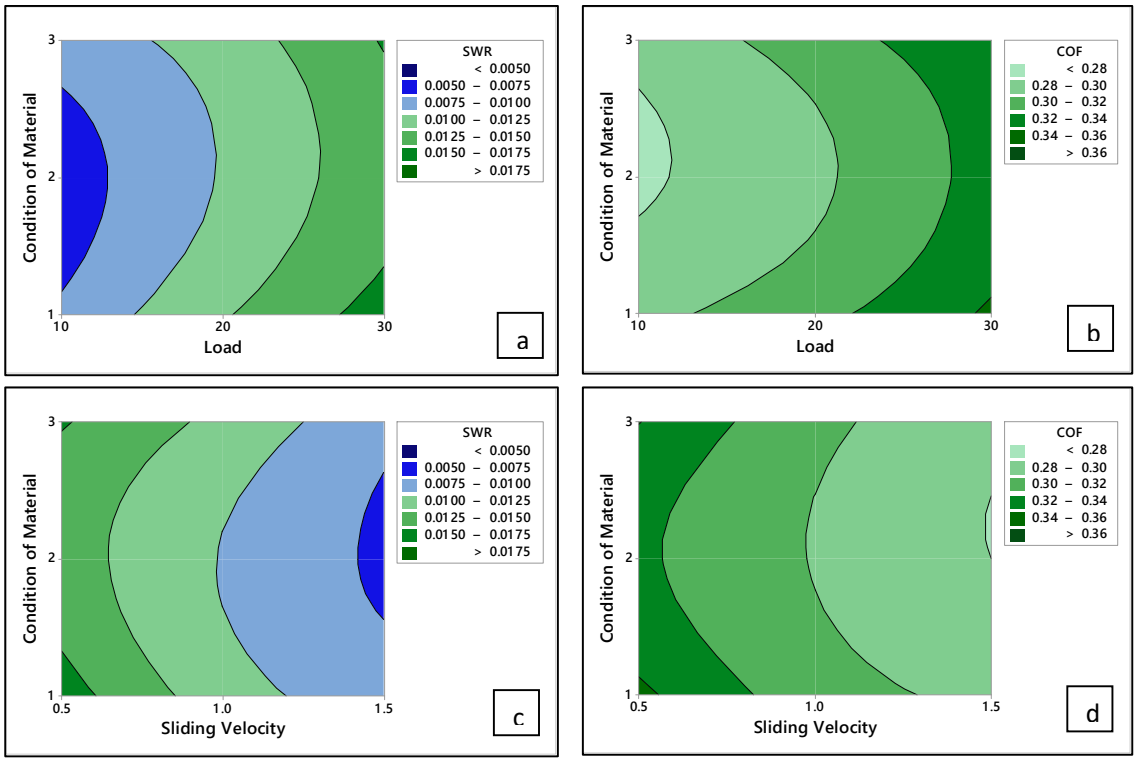

Fig 7. Variations in output responses of hybrid nanocomposite (a-b) with respect to applied load and material condition (c-d) with respect to velocity and material condition

Fig 6(a-b) shows the effect of load and material condition on the SWR and CoF of unreinforced alloy; while Fig 6(c-d) depicts the influence of velocity and material condition on the SWR and CoF of the unreinforced alloy. From the contour plots, it can be observed that for an unreinforced alloy, the minimum wear rate occurs in the regions of low load, high velocity and the material condition as artificially aged (T_6). Similarly, Fig 7(a-b) shows the effect of load and material condition on the SWR and CoF of hybrid nanocomposite while Fig 7(c-d) depicts the effect of sliding velocity and material condition on the SWR and CoF of the hybrid nanocomposite. The presence of a blue region in the contour plot manifests the minimum wear rate is observed for hybrid nanocomposite under T_6 condition. The presence of a lower applied load and higher sliding velocity also ensures the minimum wear rate for hybrid nanocomposite. A similar trend is also observed for the CoF of the hybrid nanocomposite.

4. Multi Response Optimisation using Desirability Function

Derringer and Suich [21] had developed the desirability function approach for multi-response optimisation problems. They quoted the desirability function D(x) transforms the individual response into a corresponding scale-free composite desirability. This optimisation approach uses any of the three objective functions: "the smaller-the-better (STB), the larger-the-better (LTB) and nominal-the-better (NTB)". The desirability functions should be selected based on the type of response criterion. The desirability values lie in the range of 0 to 1. The value that approaches unity indicates that the output response reaches the target. The load, sliding velocity and pin material condition were taken as input parameters, while the SWR and CoF were considered as output responses. The desired objective functions are (i) minimisation of SWR and (ii) minimisation of CoF. Besides, the constraints specified in Table 6 must be satisfied in examining the optimum levels of input parameters.

Table 6. Optimisation constraints for desirability analysis

Responses	**Constraint**	**Unreinforced alloy**		**Hybrid nanocomposite**	
		Lower limit	**Upper limit**	**Lower limit**	**Upper limit**
Load (N)	In range	10	30	10	30
Sliding velocity (m/s)	In range	0.5	1.5	0.5	1.5
Pin material condition	In range	1	3	1	3
SWR (mm^3/m)	Minimise	0.0075	0.0300	0.0042	0.0200
COF	Minimise	0.28	0.42	0.26	0.38

The feasible solutions for minimising the SWR and CoF of unreinforced alloy and hybrid composite using individual desirability values are listed in Table 7.

Table 7. Individual and composite desirability values for aluminium alloy and hybrid composite

Parameters			Unreinforced alloy			Hybrid nanocomposite		
L (N)	V (m/s)	C	Desirability for specific wear rate	Desirability for COF	Composite desirability	Desirability for specific wear rate	Desirability for COF	Composite desirability
10	0.5	1	0.532	0.617	0.767	0.510	0.586	0.739
10	0.5	2	0.836	0.844	0.917	0.627	0.724	0.821
10	0.5	3	0.647	0.737	0.840	0.533	0.639	0764
10	1	1	0.700	0.683	0.830	0.734	0.769	0.867
10	1	2	0.997	0.910	0.969	0.850	0.907	0.937
10	1	3	0.815	0.802	0.898	0.756	0.823	0.888
10	1.5	1	0.867	0.749	0.887	0.957	0.836	0.946
10	1.5	2	1.000	0.988	0.992	1.000	0.987	0.993
10	1.5	3	0.982	0.868	0.951	0.980	0.889	0.966
20	0.5	1	0.252	0.411	0.591	0.277	0.299	0.537
20	0.5	2	0.556	0.637	0.780	0.394	0.437	0.644
20	0.5	3	0.367	0.530	0.685	0.299	0.353	0.570
20	1	1	0.420	0.537	0.703	0.501	0.560	0.728
20	1	2	0.723	0.763	0.866	0.617	0.698	0.810
20	1	3	0.535	0.656	0.783	0.523	0.614	0.753
20	1.5	1	0.587	0.664	0.798	0.724	0.705	0.845
20	1.5	2	0.891	0.890	0.944	0.841	0.843	0.917
20	1.5	3	0.702	0.783	0.869	0.746	0.758	0.867
30	0.5	1	0.000	0.056	0.000	0.044	0.013	0.153
30	0.5	2	0.276	0.283	0.530	0.160	0.150	0.394
30	0.5	3	0.087	0.175	0.373	0.066	0.066	0.257
30	1	1	0.140	0.244	0.450	0.267	0.351	0.554
30	1	2	0.443	0.470	0.679	0.384	0.489	0.658
30	1	3	0.255	0.363	0.568	0.290	0.405	0.585
30	1.5	1	0.307	0.431	0.620	0.491	0.574	0.728
30	1.5	2	0.611	0.657	0.801	0.607	0.712	0.811
30	1.5	3	0.422	0.550	0.710	0.513	0.627	0.753

For unreinforced alloy, the maximum desirability value 1.000 was observed for SWR at the input parameter setting: 10 N applied load, 1.5 m/s sliding velocity and T_6 condition of the material. Similarly, the maximum desirability value of 0.988 was observed for CoF at the same input parameter setting. For hybrid nanocomposite, the maximum desirability value of 1.000 was obtained for the SWR at an applied load of 10 N, 1.5 m/s sliding velocity and T_6 material condition. The maximum desirability value of 0.987 was obtained for CoF of hybrid

nanocomposite at the same parameter setting. The contour plots of desirability values for aluminium alloy and hybrid composite are shown in Fig 8 and Fig 9 respectively.

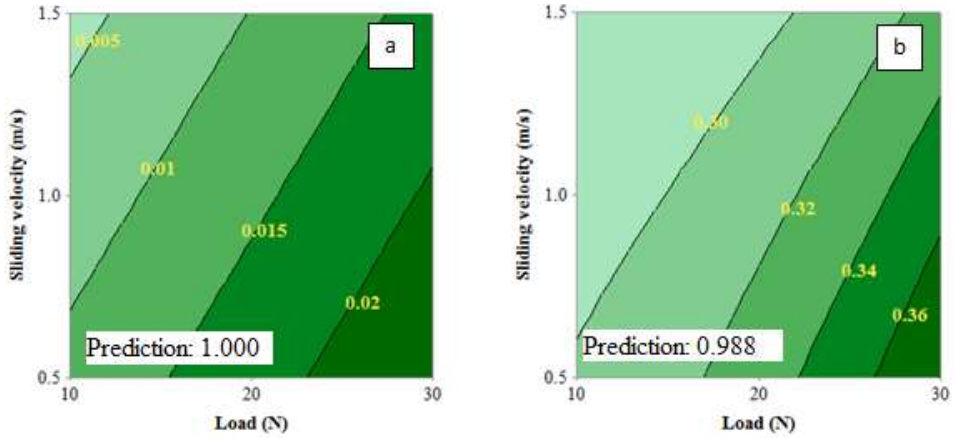

Fig 8. Contour graph at individual desirability values (a) specific wear rate (b) COF for unreinforced alloy under T_6

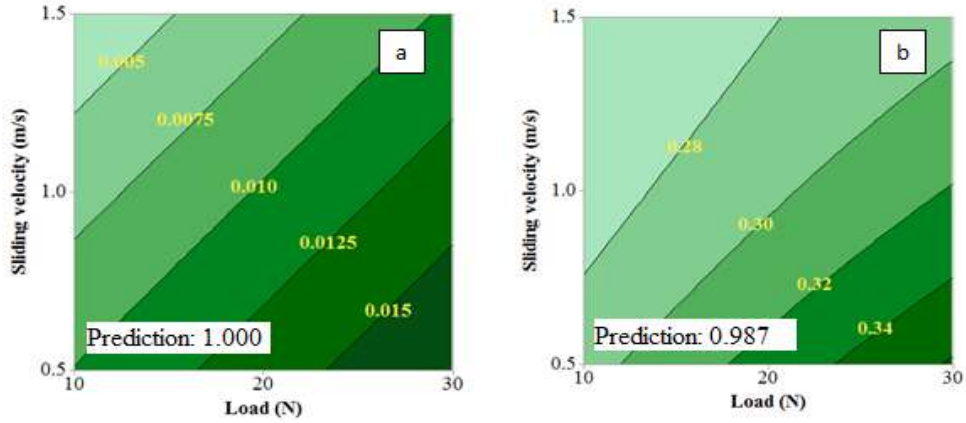

Fig 9. Contour graph at individual desirability values (a) specific wear rate (b) COF for hybrid nanocomposite under T6

In the present work, the overall desirability value is calculated from restructured response functions. Eqn. 2 is used for calculating the overall desirability value

$$D\ (x) = \ (d_1^{w1} d_2^{w2} \dots d_n^{wn})^{\frac{1}{\Sigma w^i}} \qquad (2)$$

Where d_i - individual desirability functions; n - number of objectives; w_i – weights of individual objectives. The individual desirabilities are combined in such a way to obtain geometric mean which gives the composite desirability D(x). The individual and composite

desirability values are shown in Table 6, while the corresponding multi-objective optimisation plots are presented in Fig 10 and Fig 11 respectively.

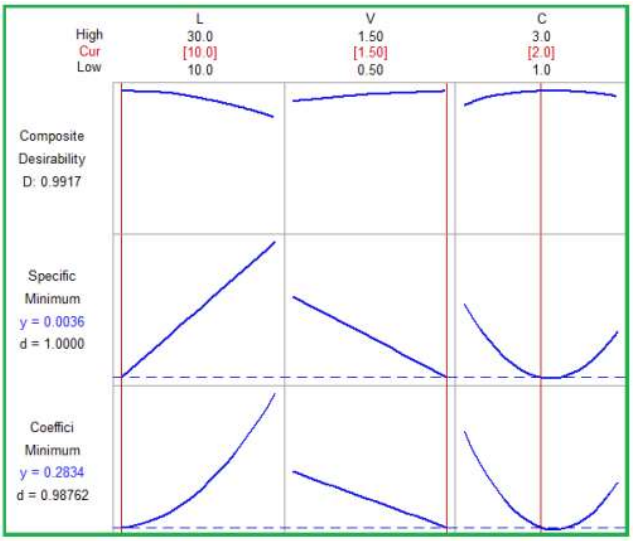

Fig 10. Multi-objective optimization plot for unreinforced alloy

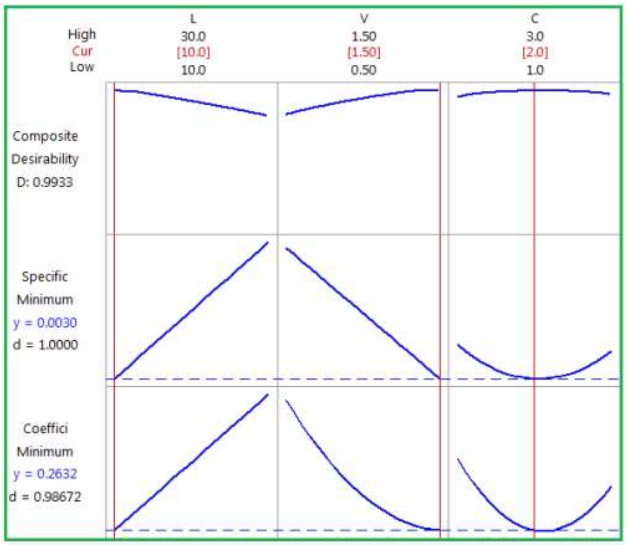

Fig 11. Multi-objective optimization plot for hybrid nanocomposite

The maximum desirability was achieved for hybrid nanocomposite under T_6 treatment. Archard established a relationship between the hardness and wear rate of material as shown in Eqn. 3

$$Q = K\frac{W}{H} \tag{3}$$

Where Q is the specific wear rate (mm^3/km), W is the volume of worn material per distance, K is constant called wear coefficient and H is the hardness of the specimen in Vickers scale (kg/mm^2).

The specific wear rate could be considerably reduced by replacing unreinforced aluminium alloy by a hybrid nanocomposite. Further, the heat treatments adopted on the hybrid nanocomposite revealed that almost 63% and 59% reduction in specific wear rate could be achieved under T_6 and DCT. The wear resistance of composite subjected to DCT was found to intermediate of as-cast and T_6. The literature revealed that additional GP zones generated during DCT are responsible for this improved wear-resistant behaviour [22]. In a similar manner, about 12% and 8% reduction in COF were reported for hybrid nanocomposite under T_6 and DCT over as-cast unreinforced aluminium alloy. These experimental results affirmed the maximum desirability value obtained for hybrid nanocomposite under T_6 through multi-objective optimization.

The maximum desirability is achieved at same parameter setting (10N, 1.5 m/s and T6 heat treatment condition) for both unreinforced alloy and hybrid nanocomposite. The penetration of hard asperities of counterface material into the softer pin material gets accelerated with increasing load. As sliding velocity increases, the tribolayer formation and strain hardening get quicken up that substantially reduce the wear loss. T_6 heat treatment is found to result in higher hardness than as-cast and DCT. This might be imputed to improved wear resistance characteristics. Thus, the mitigation of wear loss necessitates a low level of applied load, high level of sliding velocity and material condition as T_6. The experimental results also revealed the potential of hybrid nanocomposite in reducing the specific wear rate and coefficient of friction to the maximum extent than unreinforced aluminium alloy under this optimized parameter setting.

4.1. Confirmation Experiment

The confirmation experiments were conducted to affirm the optimal levels of the parameters obtained through desirability analysis. The outcomes of confirmation experiments are given in Table 8. Based on the validation experiments performed on unreinforced alloy and hybrid nanocomposite, % error were estimated and found to lie in between 1.49 - 7.67%. The accuracy of the developed statistical model was thus validated.

Table 8. Outcomes of confirmation experiments

Material	Responses	Predicted value	Experimental value	% Error
Unreinforced alloy	SWR	0.00493	0.00534	7.67
	CoF	0.283	0.298	5.03
Hybrid nanocomposite	SWR	0.00362	0.00392	7.65
	CoF	0.263	0.267	1.49

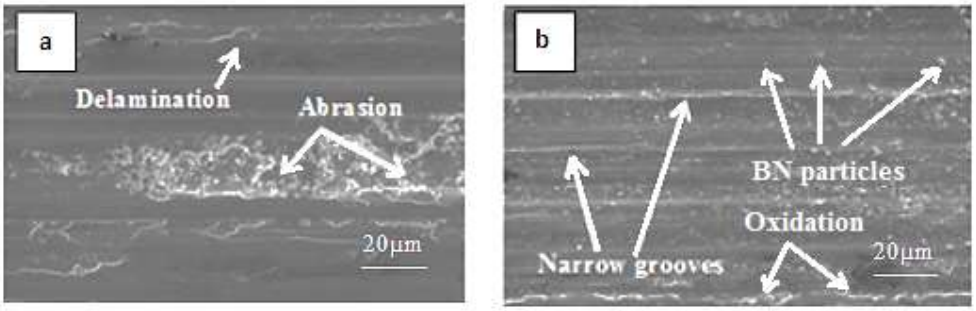

Fig 12. SEM images taken on worn-out surfaces of (a) unreinforced alloy and (b) hybrid composite under optimized conditions

The SEM images taken on worn-out surfaces of investigated materials under optimized condition are shown in Fig 12. Delamination and abrasion were found to be dominant in the case of unreinforced alloy, while no severe damaged regions were observed in the hybrid nanocomposite. The wear was considerably lower in hybrid nanocomposite under T_6 treatment, which might be imputed to the improved hardness over other material conditions (as-cast and deep cryogenic treatment). Besides, the formation of tribolayer, which eventually reduces the metal-to-metal contact between the sliding surfaces [23]. Pulling off BN particles happened in the composite was attributing to the smoother worn-out surface due to this solid lubricant film. No evidence of solid lubricant film failure was observed during the entire investigation as the sliding velocity is not exceeding the critical velocity for aluminium based composites [24]. The oxide layer formed at the surface of T_6 treated hybrid nanocomposite may be ascribed to the improved wear characteristics of nanocomposite at higher sliding velocities.

In this work, Al 7075 based hybrid nanocomposite (1% Al_2O_3 and 0.5% BN by wt.) was developed through a novel molten salt processing technique. The tribological performance of developed hybrid nanocomposite is compared with those of Al 7075 based single reinforced composites to understand the impact of hybridization. Under the identical operating conditions, the specific wear rate could be further reduced by about 17% and 23% on comparing to single reinforcement composites viz. Al 7075-Al_2O_3 and Al 7075-TiC composites [7,25].

5. Conclusions

A mathematical modelling and optimization work is carried out to assess the tribological behaviour of Al 7075 based hybrid nanocomposites. The research work results in the following findings:

- The hybrid nanocomposite exhibited better wear resistance and a lower coefficient of friction under T_6 treatment than the other two conditions considered in this investigation.
- The coefficient of friction of unreinforced aluminium alloy (Al 7075) is reduced by about 18.5% by with the incorporation of 0.5 wt.% BN and 1 wt.% Al_2O_3 nanoparticles reinforcement.
- The specific wear rate is reduced by about 63% and 59% under T_6 and DCT condition than unreinforced aluminium alloy under as-cast condition. The additional GP zones generated during these heat treatments are responsible for the improved wear resistance.
- For unreinforced Al 7075 alloy, the load is found to be a dominant parameter in determining the SWR and CoF of unreinforced Al 7075 while the contribution of other parameters viz. sliding velocity and material condition of the pin are nominal.
- In the case of hybrid nanocomposite, both load and sliding velocity are found to be majorly influencing the SWR and CoF; while the condition of the material has an insignificant effect.
- Under different operating conditions, the hybrid nanocomposite is found to be performing better than the unreinforced alloy. The multi-objective optimization discloses the preferred level for operating parameters of hybrid nanocomposite as 1-3-2 (10N, 1.5 m/s and T_6 condition)

The experimentation, subsequent mathematical modelling and optimization executed on Al 7075/1 wt.% Al_2O_3/0.5 wt.% BN nanocomposite discloses the suitability of this composite for the tribological applications of the automotive sector.

References

1. Casati R, Vedani M. Metal matrix composites reinforced by nano-particles - a review. Metals. 2014; 4(1):65-83.
2. Bodunrin MO, Alaneme KK, Chown LH. Aluminium matrix hybrid composites: a review of reinforcement philosophies; mechanical, corrosion and tribological characteristics. Journal of materials research and technology. 2015; 4(4):434-45.

3. Muley AV, Aravindan S, Singh IP. Mechanical and tribological studies on nano particles reinforced hybrid aluminum based composite. Manufacturing Review. 2015; 2:26.
4. El-Mahallawi IS, Shash AY, Amer AE. Nanoreinforced cast Al-Si alloys with Al_2O_3, TiO_2 and ZrO_2 nanoparticles. Metals. 2015; 5(2):802-21.
5. Ezatpour HR, Parizi MT, Sajjadi SA, Ebrahimi GR, Chaichi A. Microstructure, mechanical analysis and optimal selection of 7075 aluminum alloy based composite reinforced with alumina nanoparticles. Materials Chemistry and Physics. 2016; 178:119-27.
6. Su H, Gao W, Feng Z, Lu Z. Processing, microstructure and tensile properties of nano-sized Al_2O_3 particle reinforced aluminum matrix composites. Materials & Design (1980-2015). 2012; 36:590-6.
7. Veeravalli RR, Nallu R, Mohiuddin SM. Mechanical and tribological properties of AA7075–TiC metal matrix composites under heat treated (T_6) and cast conditions. Journal of Materials Research and Technology. 2016; 5(4):377-83.
8. Iacob G, Ghica VG, Buzatu M, Buzatu T, Petrescu MI. Studies on wear rate and micro-hardness of the Al/Al_2O_3/Gr hybrid composites produced via powder metallurgy. Composites Part B: Engineering. 2015; 69:603-11.
9. Baradeswaran A, Perumal AE. Study on mechanical and wear properties of Al 7075/Al_2O_3/graphite hybrid composites. Composites Part B: Engineering. 2014; 56:464-71.
10. Chen C, Guo L, Luo J, Hao J, Guo Z, Volinsky AA. Aluminum powder size and microstructure effects on properties of boron nitride reinforced aluminum matrix composites fabricated by semi-solid powder metallurgy. Materials Science and Engineering: A. 2015; 646:306-14.
11. Gorshenkov MV, Kaloshkin SD, Tcherdyntsev VV, Danilov VD, Gulbin VN. Dry sliding friction of Al-based composites reinforced with various boron-containing particles. Journal of alloys and compounds. 2012; 536:S126-9.
12. Kannan C, Ramanujam R. Effectiveness evaluation of molten salt processing and ultrasonic cavitation techniques during the production of aluminium based hybrid nanocomposites-an experimental investigation. Journal of Alloys and Compounds. 2018; 751:183-93.
13. Kannan C, Ramanujam R. Mechanical and tribological behaviour of molten salt processed self-lubricated aluminium composite under different treatments. Materials Research Express. 2018; 5(5):055040.

14. Madhukar P, Selvaraj N, Rao CS, Mishra SK. Fabrication of Light Weight Metal Matrix Nanocomposites Using Ultrasonic Cavitation Process: A State of Review. In Materials Science Forum 2019 (Vol. 969, pp. 882-888). Trans Tech Publications Ltd.
15. Xuan Y, Nastac L. The role of ultrasonic cavitation in refining the microstructure of aluminum based nanocomposites during the solidification process. Ultrasonics. 2018; 83:94-102.
16. Rajmohan T, Palanikumar K, Ranganathan S. Evaluation of mechanical and wear properties of hybrid aluminium matrix composites. Transactions of nonferrous metals society of China. 2013; 23(9):2509-17.
17. Prasad DS, Shoba C, Ramanaiah N. Investigations on mechanical properties of aluminum hybrid composites. Journal of Materials Research and Technology. 2014; 3(1):79-85.
18. Müller F, Monaghan J. Non-conventional machining of particle reinforced metal matrix composite. International Journal of Machine Tools and Manufacture. 2000; 40(9):1351-66.
19. Kok M. Abrasive wear of Al_2O_3 particle reinforced 2024 aluminium alloy composites fabricated by vortex method. Composites Part A: applied science and manufacturing. 2006; 37(3):457-64.
20. Tjong SC, Lau KC, Wu SQ. Wear of Al-based hybrid composites containing BN and SiC particulates. Metallurgical and Materials Transactions A. 1999; 30(9):2551-5.
21. Derringer G, Suich R. Simultaneous optimization of several response variables. Journal of quality technology. 1980; 12(4):214-9.
22. Franco Steier V, Ashiuchi ES, Reißig L, Araújo JA. Effect of a deep cryogenic treatment on wear and microstructure of a 6101 aluminum alloy. Advances in Materials Science and Engineering. Jun 30;2016.
23. Rohatgi PK, Tabandeh-Khorshid M, Omrani E, Lovell MR, Menezes PL. Tribology of metal matrix composites. In Tribology for scientists and engineers 2013 (pp. 233-268). Springer, New York, NY.
24. Omrani E, Moghadam AD, Menezes PL, Rohatgi PK. Influences of graphite reinforcement on the tribological properties of self-lubricating aluminum matrix composites for green tribology, sustainability, and energy efficiency—a review. The International Journal of Advanced Manufacturing Technology. 2016; 83(1-4):325-46.
25. Al-Salihi HA, Mahmood AA, Alalkawi HJ. Mechanical and wear behavior of AA7075 aluminum matrix composites reinforced by Al_2O_3 nanoparticles. Nanocomposites. 2019; 5(3):67-73.